Baseband Equivalent Models and Digital Predistortion for Mitigating Dynamic Continuous-Time Perturbations in Phase-Amplitude Modulation-Demodulation Schemes [*]

Omer Tanovic [†], Alexandre Megretski[†], Yan Li [‡]
Vladimir M. Stojanovic [§], and Mitra Osqui [¶]

August 24, 2018

Abstract

We consider baseband equivalent representation of transmission circuits, in the form of a nonlinear dynamical system $\mathbf{S}$ in discrete time (DT) defined by a series interconnection of a phase-amplitude modulator, a nonlinear dynamical system $\mathbf{F}$ in continuous time (CT), and an ideal demodulator. We show that when $\mathbf{F}$ is a CT Volterra series model, the resulting $\mathbf{S}$ is a series interconnection of a DT Volterra series model of same degree and memory depth, and an LTI system with special properties. The result suggests a new, non-obvious, analytically motivated structure of digital pre-compensation of analog nonlinear distortions such as those caused by power amplifiers in digital communication systems. The baseband model and the corresponding digital compensation structure readily extend to OFDM modulation. MATLAB simulation is used to verify proposed baseband equivalent model and demonstrate effectiveness of the new compensation scheme, as compared to the standard Volterra series approach.

[†]Omer Tanovic and Alexandre Megretski are with the Laboratory for Information and Decision Systems (LIDS), Department of Electrical Engineering and Computer Science (EECS), Massachusetts Institute of Technology (MIT), Cambridge, MA 02139, USA `{otanovic,ameg}@mit.edu`

[‡]Yan Li was with the Research Laboratory of Electronics, EECS, MIT. She is now with NanoSemi Inc., Waltham, MA 02451, USA `yan.li@nanosemitech.com`

[§]Vladimir M. Stojanovic is with the Department of Electrical Engineering and Computer Sciences, University of California Berkeley, Berkeley, CA 94720, USA `vlada@berkeley.edu`

[¶]Mitra Osqui was with LIDS, EECS, MIT. She is now with Analog Devices | Lyric Labs, Cambridge, MA 02142, USA `mitra.osqui@analog.com`

1 Notation and Terminology

j is a fixed square root of -1. $\mathbb{C}$, $\mathbb{R}$, $\mathbb{Z}$ $\mathbb{N}$ are the standard sets of complex, real, integer, and positive integer numbers. X^d, for a set X, is the set of all d-typles $(x_1, \ldots, x_d)$ with $x_i \in X$. For a set S, $|S|$ denotes the number of elements in S ($|S| = \infty$ when S is not finite).

In this paper, (scalar) *CT signals* are uniformly bounded square integrable functions $\mathbb{R} \to \mathbb{R}$. The set of all CT signals is denoted by $\mathcal{L}$. n-dimensional *DT signals* are the elements of ℓ_n (or simply ℓ for $n = 1$), the set of all square summable functions $\mathbb{Z} \to \mathbb{C}^n$. For $w \in \ell$, $w[n]$ denotes the value of w at $n \in \mathbb{Z}$. In contrast, $x(t)$ refers to the value of $x \in \mathcal{L}$ at $t \in \mathbb{R}$. The Fourier transform $\mathcal{F}$ applies to both CT and DT signals. For $x \in \mathcal{L}$, its Fourier transform $X = \mathcal{F}x$ is a square integrable function $X : \mathbb{R} \to \mathbb{C}$. For $x \in \ell_n$, the Fourier transform $X = \mathcal{F}x$ is a 2π-periodic function $X : \mathbb{R} \to \mathbb{C}$, square integrable on its period.

Systems are viewed as functions $\mathcal{L} \to \mathcal{L}$, $\mathcal{L} \to \ell$, $\ell \to \mathcal{L}$, or $\ell_k \to \ell_m$. $\mathbf{G}f$ denotes the response of system $\mathbf{G}$ to signal f (even when $\mathbf{G}$ is not linear), and the *series composition* $\mathbf{K} = \mathbf{QG}$ of systems $\mathbf{Q}$ and $\mathbf{G}$ is the system mapping f to $\mathbf{Q}(\mathbf{G}f)$. A system $\mathbf{G} : L \to L$ (or $\mathbf{G} : \ell \to \ell$) is said to be *linear and time invariant* (LTI) with *frequency response* $H : \mathbb{R} \to \mathbb{C}$ when $\mathcal{F}\mathbf{G}x = H \cdot \mathcal{F}\mathbf{x}$ for all $x \in \mathcal{L}$ (respectively $x \in \ell$).

2 Introduction

In modern communications systems, with demand for high-throughput data transmission, requirements on the system linearity become more strict. This is in large part due to a combination of ever increasing signalling rates with use of more complex modulation/demodulation schemes for enhanced spectral efficiency. This in turn forces RF transmitter power amplifiers (PA) to operate over a large portion of their transfer curves, generating out of band spectral content which degrades spectral efficiency. A common way to make the PA (and correspondingly the whole signal chain) behave linearly is to back-off PA's input level, which results in reduced power efficiency [1]. This motivates the search for a method which would help increase both linearity and power efficiency. Digital compensation offers an attractive approach to designing electronic devices with superior characteristics, and it is not a surprise that it has been used in PA linearization as well. Nonlinear distortion in an analog system can be compensated with a pre-distorter or a post-compensator system. This pre-distorter inverts nonlinear behavior of the analog part, and is usually implemented as a digital system. Techniques which employ such systems are called digital predistortion (DPD) techniques, and they can produce highly linear transmitter circuits [1]-[3].

DPD structure usually depends on behavioral PA models and their baseband equivalent counterparts. First attempts to mitigate PA's nonlinear effects by employing DPD involved using simple memoryless models in order to describe PA's behavior [4]. As the signal bandwidth

has increased over time, it has been recognized that short and long memory effects play significant role in PA's behavior [5], and should be incorporated into the model. Since then several memory baseband models and corresponding predistorters have been proposed to compensate memory effects: memory polynomials [6, 7], Hammerstein and Wiener models [8], pruned Volterra series [9], generalized memory polynomials [10], dynamic deviation reduction-based Volterra models [11, 12], as well as the most recent neural networks based behavioral models [13], and generalized rational functions based models [14]. These papers emphasize capturing the whole range of the output signal's spectrum, which is proportional to the order of nonlinearity of the RF PA, and is in practice taken to be about five times the input bandwith [???]. In wideband communication systems this would make the linearization bandwidth very large, and hence would put a significant burden on the system design (e.g., would require very high-speed data converters). Since these restrictions limit applicability of conventional models in the forthcoming wideband systems (e.g. LTE-advanced), it is beneficial to investigate model dynamics when the PA's output is also limited in bandwidth. In that case DPD would ideally mitigate distortion in that frequency band, and possible adjacent channel radiation could be taken care of by applying bandpass filter to the PA's output. Such band-limited baseband model and its corresponding DPD were investigated in [15], and promising experimental results were shown. Theoretical analysis shown in [15] follows the same modeling approach as the conventional baseband models (dynamic deviation reduction-based Volterra series modeling). Due to the bandpass filtering operation applied on the PA output, long (possibly infinite) memory dynamic behavior is now present, which makes these band-limited models fundamentally different from the conventional baseband models. Hence standard modeling methods, such as memory polynomials or dynamic deviation reduction-based Volterra series modeling, might be too general to pinpoint this new structure, and also not well suited for practical implementations (long memory requirements in nonlinear models would require exponentially large number of coefficients to be implemented in e.g. look-up table models).

In this paper, we develop an explicit expression of the equivalent baseband model, when the passband nonlinearity can be described by a Volterra series model with fixed degree and memory depth. We show that this baseband model can be written as a series interconnection of a fixed degree and short memory discrete Volterra model, and a long memory discrete LTI system which can be viewed as a bank of *reconstruction filters*. In other words, we show that the underlying baseband equivalent structure alows for untangling of passband nonlinearity, of relatively short memory, and long memory requirements imposed by bandpass filtering and modulation/demodulation operation. In exact analytical representation, the above reconstruction filters exibit discontinuities at frequency values $\pm\pi$, making their unit step responses infinitely long. Nevertheless, the reconstruction filters are shown to be smooth inside the interval $(-\pi, \pi)$, and thus aproximable by low order FIR filters. Both relatively low memory/degree requirements of the nonlinear (Volterra) subsystem and good approximability by FIR filters of the linear subsystem, allow for potentially efficient hardware implementation of the corrresponding baseband model. Suggested by the derived model, we propose a non-obvious, analytically motivated structure of digital precompensation of RF PA nonlinearities.

This paper is organized as follows. In Section III we further discuss motivation for considering problem of baseband equivalent modeling and digital predistortion, and give mathematical

description of the system under consideration. Main result is stated and proven in Section IV, i.e. in this section we give an explicit expression of the equivalent baseband model. In Section V we provide some further discussion on advantages of the proposed method, and its extension to OFDM modulation. DPD design and its performance are demonstrated by MATLAB simulation results presented in Section VI.

3   Motivation and Problem Setup

In this paper, a digital compensator is viewed as a system $\mathbf{C} : \ell \to \ell$. More specifically, a *pre-compensator* $\mathbf{C} : \ell \to \ell$ designed for a device modeled by a system $\mathbf{S} : \ell \to \mathcal{L}$ (or $\mathbf{S} : \ell \to \ell$) aims to make the composition $\mathbf{SC}$, as shown on the block diagram below,

$$ \xrightarrow{\quad u \quad} \boxed{\mathbf{C}} \xrightarrow{\quad w \quad} \boxed{\mathbf{S}} \xrightarrow{\quad v \quad} $$
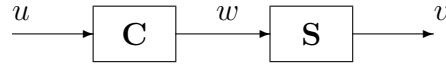
conform to a set of desired specifications. (In the simplest scenario, the objective is to make $\mathbf{SC}$ as close to the identity map as possible, in order to cancel the distortions introduced by $\mathbf{S}$.)

A common element in digital compensator design algorithms is selection of *compensator structure*, which usually means specifying a finite sequence $\tilde{\mathbf{C}} = (\mathbf{C}_1, \dots \mathbf{C}_N)$ of systems $\mathbf{C}_k : \ell \to \ell$, and restricting the actual compensator $\mathbf{C}$ to have the form

$$ \mathbf{C} = \sum_{k=1}^{N} a_k \mathbf{C}_k, \qquad a_k \in \mathbb{C}, $$

i.e., to be a linear combination of the elements of $\tilde{\mathbf{C}}$. Once the *basis* sequence $\tilde{\mathbf{C}}$ is fixed, the design usually reduces to a straightforward *least squares optimization* of the coefficients $a_k \in \mathbb{C}$.

A popular choice is for the systems $\mathbf{C}_k$ to be some *Volterra monomials*, i.e. to map their input $u = u[n]$ to the outputs $w_k = w_k[n]$ according to the polynomial formulae

$$ w_k[n] = \prod_{j=1}^{d_r(k)} \operatorname{Re} u[n - n_{k,j}^r] \prod_{j=1}^{d_i(k)} \operatorname{Im} u[n - n_{k,j}^i], $$

where the integers $d_r(k)$ and $d_i(k)$ (respectively, $n_{k,j}^r$ and $n_{k,j}^i$) will be referred to as *degrees* (respectively, *delays*). In this case, every linear combination $\mathbf{C}$ of $\mathbf{C}_k$ is a *DT Volterra series* [18], i.e., a DT system mapping signal inputs $u \in \ell$ to outputs $w \in \ell$ according to the polynomial expression

$$ w[n] = \sum_{k=1}^{N} a_k \prod_{j=1}^{d_r(k)} \operatorname{Re} u[n - n_{k,j}^r] \prod_{j=1}^{d_i(k)} \operatorname{Im} u[n - n_{k,j}^i]. $$

Selecting a proper *compensator structure* is a major challenge in compensator design: a basis which is too simple will not be capable of cancelling the distortions well, while a form that is too complex will consume excessive power and space. Having an insight into the compensator

basis selection can be very valuable. For an example (cooked up outrageously to make the point), consider the case when the ideal compensator $\mathbf{C} : u \mapsto w$ is given by

$$w[n] = \rho u[n] + \delta \left(\sum_{j=-50}^{50} u[n-j] \right)^5$$

for some (unknown) coefficients ρ and δ. One can treat $\mathbf{C}$ as a generic Volterra series expansion with fifth order monomials with delays between -50 and 50, and the first order monomial with delay 0, which leads to a basis sequence $\tilde{\mathbf{C}}$ with $1 + \binom{105}{5} = 96560647$ elements (and the same number of multiplications involved in implementing the compensator). Alternatively, one may realize that the two-element structure $\tilde{\mathbf{C}} = \{\mathbf{C}_1, \mathbf{C}_2\}$, with $w_k = \mathbf{C}_k u$ defined by

$$w_1[n] = u[n], \qquad w_2[n] = \left(\sum_{j=-50}^{50} u[n-j] \right)^5$$

is good enough.

In this paper we establish that a certain special structure is good enough to compensate for imperfect modulation. We consider modulation systems represented by the block diagram
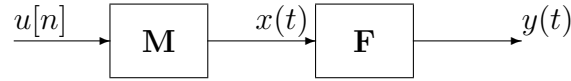
where $\mathbf{M} : \ell \to \mathcal{L}$ is the *ideal* modulator, and $\mathbf{F} : \mathcal{L} \to \mathcal{L}$ is a CT dynamical system used to represent linear and nonlinear distortion in the modulator and power amplifier circuits. We consider the ideal modulator of the form $\mathbf{M} = \mathbf{XZ}$, where $\mathbf{Z} : \ell \to \mathcal{L}$ is the *zero order hold* map $u[\cdot] \mapsto x_0(\cdot)$:

$$x_0(t) = \sum_n p(t - nT)u[n], \quad p(t) = \begin{cases} 1, & t \in [0, T), \\ 0, & t \notin [0, T) \end{cases} \tag{1}$$

with fixed sampling interval length $T > 0$ and $\mathbf{X} : \mathcal{L} \mapsto \mathcal{L}$ is the *mixer* map

$$x_0(\cdot) \mapsto x(\cdot) : \quad x(t) = 2\mathrm{Re}[\exp(j\omega_c t)x_0(t)]$$

with modulation-to-sampling frequency ratio $M \in \mathbb{N}$, i.e., with $\omega_c = 2\pi M/T$. We are particularly interested in the case when $\mathbf{F}$ is described by the *CT Volterra series model*

$$y(t) = b_0 + \sum_{k=1}^{N_b} b_k \prod_{i=1}^{\beta_k} x(t - t_{k,i}), \tag{2}$$

where $N_b \in \mathbb{N}$, $b_k \in \mathbb{R}$, $\beta_k \in \mathbb{N}$, $t_{k,i} \geq 0$ are parameters. (In a similar fashion, it is possible to consider input-output relations in which the finite sum in (2) is replaced by an integral, or an

infinite sum). One expects that the memory of $\mathbf{F}$ is not long, compared to T, i.e., that $\max t_{k,i}/T$ is not much larger than 1.

As a rule, the spectrum of the DT input $u \in \ell$ of the modulator is carefully shaped at a pre-processing stage to guarantee desired characteristics of the modulated signal $x = \mathbf{M}u$. However, when the distortion $\mathbf{F}$ is not linear, the spectrum of the $y = \mathbf{F}x$ could be damaged substantially, leading to violations of EVM and spectral mask specifications [12].

Consider the possibility of repairing the spectrum of y by pre-distorting the digital input $u \in \ell$ by a compensator $\mathbf{C} : \ell \to \ell$, as shown on the block diagram below:

$$\xrightarrow{u[n]} \boxed{\mathbf{C}} \xrightarrow{w[n]} \boxed{\mathbf{M}} \xrightarrow{x(t)} \boxed{\mathbf{F}} \xrightarrow{y(t)}$$
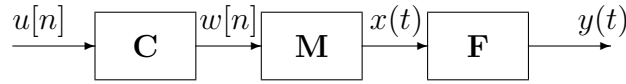
The desired effect of inserting $\mathbf{C}$ is cancellation of the distortion caused by $\mathbf{F}$. Naturally, since $\mathbf{C}$ acts in the baseband (i.e., in discrete time), there is no chance that $\mathbf{C}$ will achieve a complete correction, i.e., that the series composition $\mathbf{FMC}$ of $\mathbf{F}$, $\mathbf{M}$, and $\mathbf{C}$ will be identical to $\mathbf{M}$. However, in principle, it is sometimes possible to make the frequency contents of $\mathbf{M}u$ and $\mathbf{FMC}u$ to be identical within the CT frequency band $(\omega_c - \omega_b, \omega_c + \omega_b)$, where $\omega_b = \pi/T$ is the Nyquist frequency [19, 20]. To this end, let $\mathbf{H} : \mathcal{L} \to \mathcal{L}$ denote the ideal band-pass filter with frequency response

$$H(\omega) = \begin{cases} 1, & | \omega_c - |\omega| | < \omega_b, \\ 0, & \text{otherwise.} \end{cases} \tag{3}$$

Let $\mathbf{D} : \mathcal{L} \to \ell$ be the *ideal de-modulator* relying on the band selected by $\mathbf{H}$, i.e. the linear system for which the series composition $\mathbf{DHM}$ is the identity function. Let $\mathbf{S} = \mathbf{DHFM}$ be the series composition of $\mathbf{D}$, $\mathbf{H}$, $\mathbf{F}$, and $\mathbf{M}$, i.e. the DT system with input $w = w[n]$ and output $v = v[n]$ shown on the block diagram below:

$$\xrightarrow{w[n]} \boxed{\mathbf{M}} \xrightarrow{x(t)} \boxed{\mathbf{F}} \xrightarrow{y(t)} \boxed{\mathbf{H}} \xrightarrow{z(t)} \boxed{\mathbf{D}} \xrightarrow{v[n]}$$
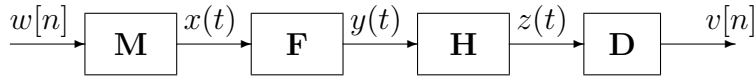
Figure 1: Block diagram of $\mathbf{S} = \mathbf{DHFM}$

By construction, the ideal compensator $\mathbf{C}$ should be the inverse $\mathbf{C} = \mathbf{S}^{-1}$ of $\mathbf{S}$, as long as the inverse does exist.

A key question answered in this paper is "what to expect from system $\mathbf{S}$?" If one assumes that the continuous-time distortion subsystem $\mathbf{F}$ is simple enough, what does this say about $\mathbf{S}$?

This paper provides an explicit expression for $\mathbf{S}$ in the case when $\mathbf{F}$ is given in the CT Volterra series form (2) with *degree* $d = \max \beta_k$ and *depth* $t_{max} = \max t_{k,i}$. The result reveals that, even though $\mathbf{S}$ tends to have infinitely long memory (due to the ideal band-pass filter $\mathbf{H}$ being involved in the construction of $\mathbf{S}$), it can be represented as a series composition $\mathbf{S} = \mathbf{LV}$, where $\mathbf{V} : \ell \to \ell_N$ maps scalar complex input $w \in \ell$ to real vector output $g \in \ell_N$ in such a

way that the k-th scalar component $g_k[n]$ of $g[n] \in \mathbb{R}^N$ is given by

$$g_k[n] = \prod_{i=0}^{m}(\text{Re } w[n-i])^{\alpha_i} \prod_{i=0}^{m}(\text{Im } w[n-i])^{\beta_i}, \qquad \alpha_i, \beta_i \in \mathbb{Z}_+, \qquad \sum_{i=0}^{m}\alpha_i + \sum_{i=0}^{m}\beta_i \le d,$$

m is the minimal integer not smaller than t_{max}/T, and $\mathbf{L} : \ell_N \to \ell$ is an LTI system.
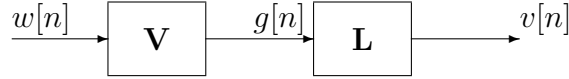

Figure 2: Block diagram of the structure of $\mathbf{S}$

Moreover, $\mathbf{L}$ can be shown to have a good approximation of the form $\mathbf{L} \approx X\mathbf{L}_0$, where X is a static gain matrix, and $\mathbf{L}_0$ is an LTI model which does not depend on b_k and $t_{k,i}$. In other words, $\mathbf{S}$ can be well approximated by combining a Volterra series model with a short memory, and a *fixed* (long memory) LTI, as long as the memory depth t_{max} of $\mathbf{F}$ is short, relative to the sampling time T.

In most applications, with an appropriate scaling and time delay, the system $\mathbf{S}$ to be inverted can be viewed as a small perturbation of identity, i.e. $\mathbf{S} = \mathbf{I} + \Delta$. When Δ is "small" in an appropriate sense (e.g., has small incremental L2 gain $\|\Delta\| \ll 1$), the inverse of $\mathbf{S}$ can be well approximated by $\mathbf{S}^{-1} \approx \mathbf{I} - \Delta = 2\mathbf{I} - \mathbf{S}$. Hence the result of this paper suggests a specific structure of the compensator (pre-distorter) $\mathbf{C} \approx \mathbf{I} - \Delta = 2\mathbf{I} - \mathbf{S}$. In other words, a plain Volterra monomials structure is, in general, not good enough for $\mathbf{C}$, as it lacks the capacity to implement the long-memory LTI post-filter $\mathbf{L}$. Instead, $\mathbf{C}$ should be sought in the form $\mathbf{C} = \mathbf{I} - \mathbf{L_0}X\mathbf{V}$, where $\mathbf{V}$ is the system generating all Volterra series monomials of a limited depth and limited degree, $\mathbf{L}_0$ is a *fixed* LTI system with a very long time constant, and X is a matrix of coefficients to be optimized to fit the data available.

3.1 Ideal Demodulator

In digital communications literature, demodulation is usually described as downconvertion of the passband signal, followed by low-pass filtering (LPF) and sampling [21].Often, the low-pass filtering (windowing) operation in the transmitter (i.e. in the modulation part of the system) is obtain with a filter whose frequency response has significant spectral content outside of band of interest (i.e. significant side-lobes are present). In that case the LPF operation after down-conversion, in demodulator, would null a significant portion of the input signal's spectrum, thus introducing additional distortion in the **DHFM** signal chain. Thus distortions introduced by the non-ideal demodulation could mask a possibly good preformance of the digital predistor-tion. For that reason, in this paper, we apply demodulation which completely recovers the input signal, without introducing additional distortion. We call this operation *ideal demodulation*, and in the following derive corresponding mathematical model.

The most commonly known expression for the ideal demodulator inverts not $\mathbf{M} = \mathbf{XZ}$ but $\mathbf{M}_0 = \mathbf{XH}_0\mathbf{Z}$, i.e., the modulator which inserts $\mathbf{H}_0$, the *ideal low-pass filter* for the baseband, between zero-order hold $\mathbf{Z}$ and mixer $\mathbf{X}$, where $\mathbf{H}_0$ is the CT LTI system with frequency response

$$H_0(\omega) = \begin{cases} 1, & |\omega| < \omega_b, \\ 0, & \text{otherwise.} \end{cases}$$

Specifically, let $\mathbf{X}_c : \mathcal{L} \mapsto \mathcal{L}$ be the *dual mixer* mapping $x(\cdot)$ to $e(t) = \exp(-j\omega_c t)x(t)$. Let $\mathbf{E} : \mathcal{L} \mapsto \ell$ be the *sampler*, mapping $g(\cdot)$ to $w[n] = g(nT)$. Finally, let $\mathbf{A}_0$ be the DT LTI system with frequency response A_0 defined by

$$A_0(\Omega) = P(\Omega/T)^{-1} \quad \text{for} \quad |\Omega| < \pi,$$

where P is the Fourier transform of $p = p(t)$ (1). Then the composition $\mathbf{A}_0\mathbf{EH}_0\mathbf{X}_c\mathbf{HM}_0$ is an identity map. Equivalently, $\mathbf{A}_0\mathbf{EH}_0\mathbf{X}_c$ is the ideal demodulator for $\mathbf{M}_0$.

For the modulation map $\mathbf{M} = \mathbf{XZ}$ considered in this paper, the ideal demodulator has the form $\mathbf{AEH}_0\mathbf{X}_c$, where $\mathbf{A} : \ell \mapsto \ell$ is the linear system mapping $w \in \ell(\mathbb{C})$ to $s \in \ell(\mathbb{C})$ according to

$$\text{Re}(s) = \mathbf{A}_{rr}\text{Re}(w) + \mathbf{A}_{ri}\text{Im}(w),$$

$$\text{Im}(s) = \mathbf{A}_{ir}\text{Re}(w) + \mathbf{A}_{ii}\text{Im}(w),$$

and $\mathbf{A}_{rr}$, $\mathbf{A}_{ri}$, $\mathbf{A}_{ir}$, $\mathbf{A}_{ii}$ are LTI systems with frequency responses $A_{rr} = (P_0 - P_i)Q$, $A_{ir} = A_{ri} = -P_q Q$, $A_{ii} = (P_0 + P_i)Q$, where $Q = (P_0^2 - P_i^2 - P_q^2)^{-1}$, $P_i = (P^+ + P^-)/2$, $P_q = (P^+ - P^-)/2j$, and $P_0, P^+, P^- \in \mathcal{L}_{2\pi}$ are defined for $|\Omega| < \pi$ by

$$P_0(\Omega) = P(\Omega/T), \; P^+(\Omega) = P_0(\Omega + \theta), \; P^-(\Omega) = P_0(\Omega - \theta)$$

with $\theta = 4\pi M$.

4   Main Result

Before stating the main result of this paper, let us introduce some additional notation. For $d \in \mathbb{N}$ and $\tau = (\tau_1, \ldots, \tau_d) \in [0, \infty)^d$ let $\mathbf{F}_\tau : \mathcal{L} \to \mathcal{L}$ be the CT system mapping inputs $x \in \mathcal{L}$ to the outputs $y \in \mathcal{L}$ according to

$$y(t) = x(t - \tau_1)x(t - \tau_2)\ldots x(t - \tau_d).$$

In the rest of this section, many expressions will contain products of the above type, where the complex-valued signal x can be written as $x = i + j \cdot q$, with i and q representing its real and imaginary part, respectively. It follows that the corresponding products would range over delayed real and imaginary parts of x. As will be shown later (e.g. in (8)), these product factors can be classified into four groups: combinations of delayed or un-delayed, real or imaginary part of x. This explains appearance of the index set $\{1, 2, 3, 4\}$ which will be used to encode these four groups of signals.

For every $\mathbf{m} = (m_1, \ldots, m_d) \in \{1, 2, 3, 4\}^d$ and integer $l \in \{1, 2, 3, 4\}$ let $S_\mathbf{m}^l$ be the set of all indices i for which $m_i = l$, i.e., $S_\mathbf{m}^l = \{i \in \{1, \ldots, d\} : m_i = l\}$. Furthermore, define

$$N_\mathbf{m}^1 = |S_\mathbf{m}^1 \cup S_\mathbf{m}^2|, \quad N_\mathbf{m}^2 = |S_\mathbf{m}^3 \cup S_\mathbf{m}^4|.$$

Clearly $N_\mathbf{m}^1 + N_\mathbf{m}^2 = d$ for every $\mathbf{m} \in \{1, 2, 3, 4\}^d$. Let $R_\mathbf{m}^c = \{-1, 1\}^{N_\mathbf{m}^1}$ and $R_\mathbf{m}^s = \{-1, 1\}^{N_\mathbf{m}^2}$. Let $(\cdot, \cdot) : \mathbb{R}^d \times \mathbb{R}^d \to \mathbb{R}$ denote the standard scalar product in $\mathbb{R}^d$. Define the maps $\tilde{\sigma}, \sigma : \mathbb{R}^d \to \mathbb{R}$ by $\tilde{\sigma}(x) = \sum_{i=1}^d x_i$ and $\sigma(x) = \tilde{\sigma}(x) - 1$. For a given $m \in \{1, 2, 3, 4\}^d$ and $x \in \mathbb{R}^d$ let $\pi_\mathbf{m}(x)$ be the product of all x_i with $i \in S_\mathbf{m}^3 \cup S_\mathbf{m}^4$. For $i \in \{1, 2\}$, define projection operators $\mathcal{P}_\mathbf{m}^i : \mathbb{R}^d \to \mathbb{R}^{N_\mathbf{m}^i}$ by

$$\mathcal{P}_\mathbf{m}^i x = \begin{bmatrix} x_{n_1} & \cdots & x_{n_{N_\mathbf{m}^i}} \end{bmatrix}^T, \quad \{n_1, \ldots, n_{N_\mathbf{m}^i}\} = S_\mathbf{m}^{2i-1} \cup S_\mathbf{m}^{2i}, \quad n_1 < \cdots < n_{N_\mathbf{m}^i}.$$

The following example should elucidate the above, somewhat involved, notation. Let $d = 7$ and $\mathbf{m} = (3, 1, 4, 2, 1, 3, 1)$. Then

$$S_\mathbf{m}^1 = \{2, 5, 7\}, \quad S_\mathbf{m}^2 = \{4\}, \quad S_\mathbf{m}^3 = \{1, 6\}, \quad S_\mathbf{m}^4 = \{3\},$$

$$N_\mathbf{m}^1 = |S_\mathbf{m}^1 \cup S_\mathbf{m}^2| = 4, \quad N_\mathbf{m}^2 = |S_\mathbf{m}^3 \cup S_\mathbf{m}^4| = 3,$$

$$R_\mathbf{m}^c = \{-1, 1\}^4, \quad R_\mathbf{m}^2 = \{-1, 1\}^3,$$

$$\mathcal{P}_\mathbf{m}^1 x = \begin{bmatrix} x_2 & x_4 & x_5 & x_7 \end{bmatrix}^T, \quad \mathcal{P}_\mathbf{m}^2 x = \begin{bmatrix} x_1 & x_3 & x_6 \end{bmatrix}^T,$$

$$\pi_\mathbf{m}(x) = x_1 x_3 x_6.$$

Given a vector $\tau \in [0, \infty)^d$ let $\mathbf{k}$ be the unique vector in $(\mathbb{N} \cup \{0\})^d$ such that $\tau = \mathbf{k}T + \tau'$ and $\tau' \in [0, T)^d$.

Let $\theta : \mathbb{R} \to \{0, 1\}$ denote the Heaviside step function $\theta(t) = 0$ for $t < 0$, $\theta(t) = 1$ for $t \geq 0$. For $T \in (0, \infty)$ let $p(t) = p_T(t) = \theta(t) - \theta(t - T)$ denote the basic pulse shape of the zero-order hold (ZOH) system with sampling time T. Given $m \in \{1, 2, 3, 4\}^d$ and $\tau' \in [0, T)^d$ define

$$\tau_{min}^\mathbf{m} = \begin{cases} \max_{i \in S_\mathbf{m}^2 \cup S_\mathbf{m}^4} \tau_i', & |S_\mathbf{m}^2 \cup S_\mathbf{m}^4| > 0, \\ 0, & \text{otherwise,} \end{cases}$$

and

$$\tau_{max}^\mathbf{m} = \begin{cases} \min_{i \in S_\mathbf{m}^1 \cup S_\mathbf{m}^3} \tau_i', & |S_\mathbf{m}^1 \cup S_\mathbf{m}^3| > 0, \\ T, & \text{otherwise.} \end{cases}$$

Let $p_{\mathbf{m}, \tau} : \mathbb{R} \to \mathbb{R}$ be the continuous time signal defined by

$$p_{\mathbf{m}, \tau}(t) = \begin{cases} \theta(t - \tau_{min}^\mathbf{m}) - \theta(t - \tau_{max}^\mathbf{m}), & \tau_{min}^\mathbf{m} < \tau_{max}^\mathbf{m} \\ 0, & \text{otherwise,} \end{cases}. \tag{4}$$

We denote its Fourier transform by $P_{\mathbf{m}, \tau}(\omega)$.

As can be seen from (2), the general CT Volterra model is a linear combination of subsystems $\mathbf{F}_\tau$, with different τ. Thus, in order to establish the desired decomposition $\mathbf{S} = \mathbf{L}\mathbf{V}$ it is
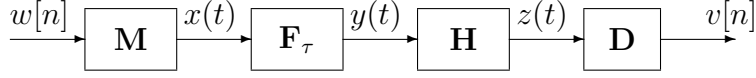
Figure 3: Block diagram of system $\mathbf{S}_\tau = \mathbf{DHF}_\tau\mathbf{M}$

sufficient to consider the case $\mathbf{S}_\tau = \mathbf{DHF}_\tau\mathbf{M}$ with a specific τ, as shown on the block diagram in Fig. 3. The following theorem gives an answer to that question.

Theorem 4.1. For $\tau \in [0, \infty)^d$, the system $\mathbf{DHF}_\tau\mathbf{M}$ maps $w \in \ell$ to

$$v = \mathbf{A}u \in \ell, \quad \text{with} \quad u = \sum_{\mathbf{m} \in \{1,2,3,4\}^d} x_{\mathbf{m},\mathbf{k}} * g_{\mathbf{m}},$$

where

$$i[n] = \mathrm{Re}(w[n]), \quad q[n] = \mathrm{Im}(w[n]),$$

$$x_{\mathbf{m},\mathbf{k}}[n] = \prod_{i \in S_{\mathbf{m}}^1} i[n - k_i - 1] \prod_{i \in S_{\mathbf{m}}^2} i[n - k_i] \prod_{i \in S_{\mathbf{m}}^3} q[n - k_i - 1] \prod_{i \in S_{\mathbf{m}}^4} q[n - k_i],$$

and the sequences (unit sample responses) $g_{\mathbf{m}} = g_{\mathbf{m}}[n]$ are defined by their Fourier transforms

$$G_{\mathbf{m}}(\Omega) = \frac{(j)^{N_{\mathbf{m}}^2}}{2^d} \sum_{r_c \in R_{\mathbf{m}}^c} \sum_{r_s \in R_{\mathbf{m}}^s} \prod_{l=1}^{N_{\mathbf{m}}^2} r_c(l) \cdot P_{\mathbf{m},\bar{\tau}}\left(\tilde{\Omega}\right) \cdot e^{-j\omega_c[(r_c, \mathcal{P}_{\mathbf{m}}^1 \bar{\tau}) + (r_s, \mathcal{P}_{\mathbf{m}}^2 \bar{\tau})]}, \tag{5}$$

$$\tilde{\Omega} = \frac{\Omega}{T} - \omega_c \sum_i r_c(i) - \omega_c \sum_l r_s(l) + \omega_c.$$

Proof. We first state and prove the following Lemma, which is a special case of Theorem 4.1, in which τ ranges over $[0, T)^d$ (instead of $\tau \in [0, \infty)^d$), and hence $\mathbf{k} = \mathbf{0}$. The proof of Theorem 4.1 follows immediately from this Lemma.

Lemma 4.2. The DT system $\mathbf{DHF}_\tau\mathbf{M}$ with $\tau \in [0, T)^d$ maps $w \in \ell$ to

$$v = \mathbf{A}u \in \ell, \quad \text{with} \quad u = \sum_{\mathbf{m} \in \{1,2,3,4\}^d} x_{\mathbf{m}} * g_{\mathbf{m}},$$

where

$$x_{\mathbf{m}}[n] = i[n-1]^{|S_{\mathbf{m}}^1|} i[n]^{|S_{\mathbf{m}}^2|} q[n-1]^{|S_{\mathbf{m}}^3|} q[n]^{|S_{\mathbf{m}}^4|}, \quad i[n] = \mathrm{Re}(w[n]), \quad q[n] = \mathrm{Im}(w[n]),$$

and the sequences $g_{\mathbf{m}}$ are as defined in Theorem 4.1.

Proof. A block diagram of system $\mathbf{DHF}_\tau\mathbf{M}$ is shown in Fig. 4, where $\mathbf{M}$ and $\mathbf{D}$ are decomposed into elementary subsystems as defined in the previous chapters. In order to prove Lemma 4.1, we first find the analytical expression of signal y as a function of w, ω_c, T and τ, and then we find the map from y to u.
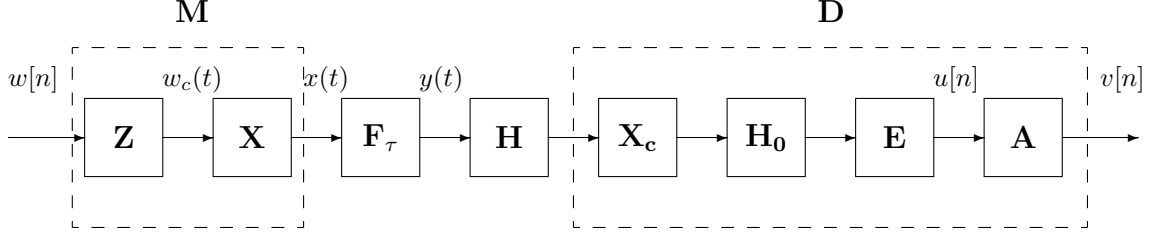
Figure 4: Block diagram of system $\mathbf{S}_\tau = \mathbf{DHF}_\tau\mathbf{M}$

Consider first the case $d = 1$ (i.e., $\mathbf{F}_\tau$ is just a delay by $\tau \in [0, T)$). By definition, the outputs w_c, x_c and y of $\mathbf{Z}$, $\mathbf{X}$ and $\mathbf{F}$ are given by

$$w_c(t) = \frac{1}{T} \sum_{n=-\infty}^{\infty} w[n]p(t - nT) = \underbrace{\frac{1}{T} \sum_{n=-\infty}^{\infty} i[n]p(t - nT)}_{i_c(t)} + \underbrace{\frac{j}{T} \sum_{n=-\infty}^{\infty} w[n]p(t - nT)}_{jq_c(t)}.$$

$$x(t) = (\mathbf{X}w_c)(t) = \mathrm{Re}\{\exp(j\omega_c t)w_c(t)\},$$

$$y(t) = i_c(t - \tau)\cos(\omega_c t - \omega_c \tau) - q_c(t - \tau)\sin(\omega_c t - \omega_c \tau). \tag{6}$$

Consider the representation $p(t) = p_{1,\tau}(t) + p_{2,\tau}(t)$, where

$$p_{1,\tau}(t) = \theta(t) - \theta(t - \tau), \qquad p_{2,\tau}(t) = \theta(t - \tau) - \theta(t - T).$$

Let $\mathbf{Z_1} : \ell(\mathbb{C}) \to \mathcal{L}(\mathbb{C})$ and $\mathbf{Z_2} : \ell(\mathbb{C}) \to \mathcal{L}(\mathbb{C})$ be the digital-to-analog converters with pulse shapes $p_{1,\tau}$ and $p_{2,\tau}$ respectively. Let $\mathbf{B}$ denote the backshift function mapping $x \in \ell$ to $y = \mathbf{B}x \in \ell$, defined by $y[n] = x[n - 1]$. Then

$$\begin{aligned} i_c(t - \tau) &= e_{1,\tau}(t) + e_{2,\tau}(t), \\ q_c(t - \tau) &= e_{3,\tau}(t) + e_{4,\tau}(t), \end{aligned} \tag{7}$$

where

$$e_{1,\tau} = \mathbf{Z_1}\mathbf{B}i, \quad \text{i.e.,} \quad e_{1,\tau}(t) = \frac{1}{T} \sum_{n=-\infty}^{\infty} i[n-1]p_{1,\tau}(t - nT),$$

$$e_{2,\tau} = \mathbf{Z_2}i, \quad \text{i.e.,} \quad e_{2,\tau}(t) = \frac{1}{T} \sum_{n=-\infty}^{\infty} i[n]p_{2,\tau}(t - nT),$$

$$e_{3,\tau} = \mathbf{Z_1}\mathbf{B}q, \quad \text{i.e.,} \quad e_{3,\tau}(t) = -\frac{1}{T} \sum_{n=-\infty}^{\infty} q[n-1]p_{1,\tau}(t - nT), \tag{8}$$

$$e_{4,\tau} = \mathbf{Z_2}q, \quad \text{i.e.,} \quad e_{4,\tau}(t) = -\frac{1}{T} \sum_{n=-\infty}^{\infty} q[n]p_{2,\tau}(t - nT).$$

It follows from (6)-(8), that the output $y(t)$ of $\mathbf{F}_\tau$ can be expressed as:

$$y(t) = f_1(t) + f_2(t) + f_3(t) + f_4(t),$$

where

$$f_i(t) = \begin{cases} e_{i,\tau}(t)\cos(\omega_c t - \omega_c \tau), & i = 1, 2 \\ e_{i,\tau}(t)\sin(\omega_c t - \omega_c \tau), & i = 3, 4 \end{cases}. \tag{9}$$

Therefore subsystem $\mathbf{F}_\tau \mathbf{M}$, mapping $w[n]$ to $y(t)$, can be represented as a parallel interconnection of amplitude modulated delayed and undelayed in-phase and quadrature components of $w[n]$. This is shown in Fig. 5, where $\tilde{\mathbf{D}} = \mathbf{E}\mathbf{H_0}\mathbf{X_c}\mathbf{H}$.
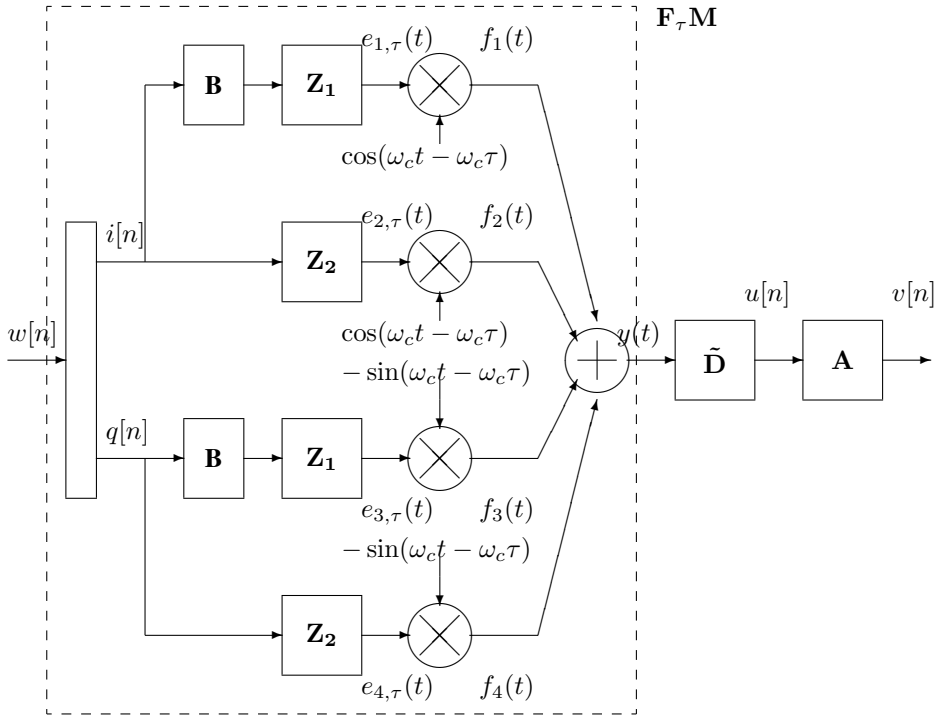

Figure 5: Equivalent representation of $\mathbf{DHF}_\tau \mathbf{M}$

Suppose now that order d of $\mathbf{F}_\tau$ is an arbitrary positive integer larger than 1, i.e. that $\mathbf{F}_\tau : x \mapsto x(t - \tau_1) \cdot \ldots \cdot x(t - \tau_d)$. Then the output y of $\mathbf{F}_\tau$ can be represented in the form

$$y(t) = [i_c(t - \tau_1)\cos(\omega_c t - \omega_c \tau_1) - q_c(t - \tau_1)\sin(\omega_c t - \omega_c \tau_1)]\cdot$$
$$\cdot [i_c(t - \tau_2)\cos(\omega_c t - \omega_c \tau_2) - q_c(t - \tau_2)\sin(\omega_c t - \omega_c \tau_2)] \cdot \ldots$$
$$\ldots \cdot [i_c(t - \tau_d)\cos(\omega_c t - \omega_c \tau_d) - q_c(t - \tau_d)\sin(\omega_c t - \omega_c \tau_d)]. \tag{10}$$

Let us denote the factors in product in (10) as $y_i(t)$, i.e.

$$y_i(t) = i_c(t - \tau_i)\cos(\omega_c t - \omega_c \tau_i) - q_c(t - \tau_i)\sin(\omega_c t - \omega_c \tau_i).$$

For each i, signal $y_i(t)$ can be represented as the output of subsystem $\mathbf{F}_{\tau_i}\mathbf{M}$, where $\mathbf{F}_\tau$ is just a simple delay, as discussed above. Therefore system $\mathbf{F}_\tau\mathbf{M}$, mapping w to y, can be represented as a parallel interconnection of d subsystems $\mathbf{F}_{\tau_i}\mathbf{M}$, with corresponding outputs y_i, where $y(t) = y_1(t) \cdot \ldots \cdot y_d(t)$. This is depicted in Fig. 6. Hence, by using the same notation as in Figs 5 and 6, signal $y(t)$ can be written as

$$y(t) = \prod_{i=1}^{d} y_i(t) = \prod_{i=1}^{d}(f_1^i(t) + f_2^i(t) + f_3^i(t) + f_4^i(t)) = \sum_{\mathbf{m}\in[4]^d} f_{m_1}^1(t) \cdot \ldots \cdot f_{m_d}^d(t). \quad (11)$$

We have

$$y(t) = \sum_{\mathbf{m}\in\{1,2,3,4\}^d} f_{\mathbf{m}}(t), \quad (12)$$

where $f_{\mathbf{m}}(t)$ denotes the product $f_{m_1}^1(t) \cdot \ldots \cdot f_{m_d}^d(t)$.

Here componenets m_i of $\mathbf{m} = (m_1, m_2, \ldots, m_d) \in \{1, 2, 3, 4\}^d$, determine which signal f_j^i, $j \in \{1, 2, 3, 4\}$ from (9) participates as a product factor in $f_{\mathbf{m}}(t)$. With signals $e_{m_i,\tau_i}(t)$ as defined in (8), it follows that summands in (12) can be written as

$$f_{\mathbf{m}}(t) = (-1)^{N_{\mathbf{m}}^2} \prod_{i=1}^{d} e_{m_i,\tau_i}(t) \cdot \prod_{k\in S_{\mathbf{m}}^1\cup S_{\mathbf{m}}^2} \cos(\omega_c t - \omega_c\tau_k) \cdot \prod_{l\in S_{\mathbf{m}}^3\cup S_{\mathbf{m}}^4} \sin(\omega_c t - \omega_c\tau_l). \quad (13)$$

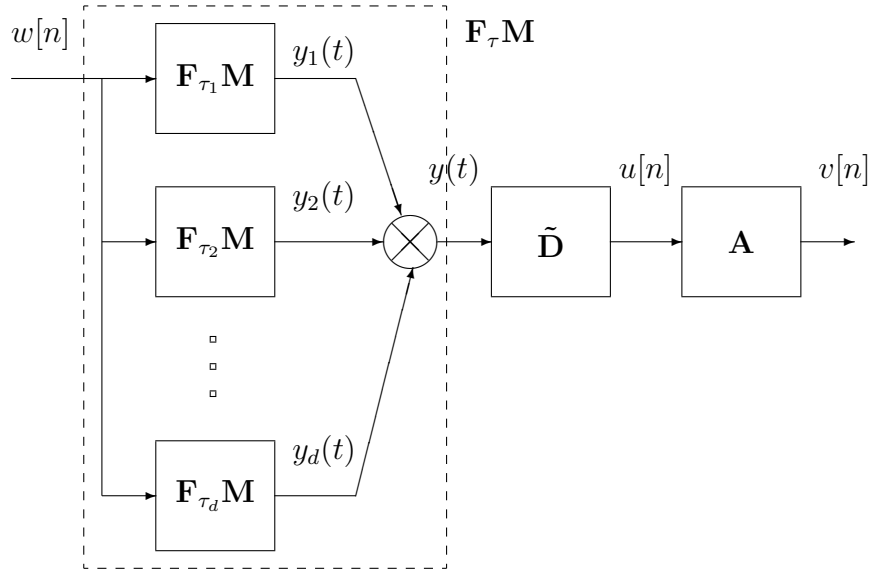

Figure 6: $\mathbf{F}_\tau\mathbf{M}$ as parallel interconnection of subsystems $\mathbf{F}_{\tau_i}\mathbf{M}$

Products of cosines and sines in (13) can be expressed as sums of complex exponents as follows

$$\prod_{k\in S_{\mathbf{m}}^1\cup S_{\mathbf{m}}^2} \cos(\omega_c t - \omega_c\tau_k) = \frac{1}{2^{N_{\mathbf{m}}^1}} \sum_{r\in R_{\mathbf{m}}^c} e^{j\omega_c\bar{\sigma}(r)t} \cdot e^{-j\omega_c(r,\mathcal{P}_{\mathbf{m}}^1\tau)}, \quad (14)$$

$$\prod_{l \in S_{\mathbf{m}}^3 \cup S_{\mathbf{m}}^4} \sin(\omega_c t - \omega_c \tau_l) = \frac{1}{(2j)^{N_{\mathbf{m}}^2}} \sum_{r \in R_{\mathbf{m}}^s} \prod_{i=1}^{N_{\mathbf{m}}^2} r(i) \cdot e^{j\omega_c \bar{\sigma}(r)t} \cdot e^{-j\omega_c(r, \mathcal{P}_m^2 \tau)}. \tag{15}$$

Recall that the signals $e_{m_i, \tau_i}(t)$ are obtained by applying pulse amplitude modulation with pulse signals $p_{1,\tau_i}(t)$ or $p_{2,\tau_i}(t)$ on in-phase or quadrature components i and q of the input signal (or their delayed counterparts $\mathbf{B}i$ and $\mathbf{B}q$). Let $e_{\mathbf{m},\tau}(t)$ be the product of signals $e_{m_i,\tau_i}(t)$ (as given in (13)). We now derive an expression for $e_{\mathbf{m},\tau}(t)$ as a function of signals $i, q, \mathbf{B}i$ and $\mathbf{B}q$. We first investigate signal $e_{\mathbf{m},\tau}(t)$ for $t \in [nT, (n+1)T)$, with $n > 1$ an integer. There are three possible cases:

(i) $S_{\mathbf{m}}^2 \cup S_{\mathbf{m}}^4 = \emptyset$, i.e. signals $e_{m_i,\tau_i}(t)$ were all obtained by applying pulse amplitude modulation with $p_{1,\tau}(t)$. It immediately follows that product $e_{\mathbf{m},\tau}(t)$ of signals $e_{m_i,\tau_i}(t)$ is nonzero only for $t \in [nT, nT + \tau_{max})$, where $\tau_{max} = \min_i \tau_i$.

(ii) $S_{\mathbf{m}}^1 \cup S_{\mathbf{m}}^3 = \emptyset$, i.e. signals $e_{m_i,\tau_i}(t)$ were all obtained by applying pulse amplitude modulation with $p_{2,\tau}(t)$. It immediately follows that product $e_{\mathbf{m},\tau}(t)$ of signals $e_{m_i,\tau_i}(t)$ is nonzero only for $t \in [nT + \tau_{min}, (n+1)T)$, where $\tau_{min} = \max_i \tau_i$.

(iii) Both $S_{\mathbf{m}}^1 \cup S_{\mathbf{m}}^3$ and $S_{\mathbf{m}}^2 \cup S_{\mathbf{m}}^4$ are non-empty. Let $\tau_{min} = \max_{i \in S_{\mathbf{m}}^2 \cup S_{\mathbf{m}}^4} \tau_i$ and $\tau_{max} = \min_{i \in S_{\mathbf{m}}^1 \cup S_{\mathbf{m}}^3} \tau_i$. It follows that $e_{\mathbf{m},\tau}(t) = 0$ for all $t \in [nT, (n+1)T)$ if $\tau_{min} > \tau_{max}$. Otherwise it is nonzero for $t \in [nT + \tau_{min}, nT + \tau_{max})$. This is depicted in Fig. 7 (for the sake of simplicity, only in-phase component i is considered, but in general signals q and $\mathbf{B}q$ would appear too).

The above discussion implies that the signal $e_{\mathbf{m},\tau}(t)$ can be expressed as

$$e_{\mathbf{m},\tau}(t) = \sum_{n=-\infty}^{\infty} x_{\mathbf{m}}[n] p_{\mathbf{m},\tau}(t - nT), \tag{16}$$

where $p_{\mathbf{m},\tau}(t)$ was defined in (4), and DT signal $x_{\mathbf{m}} = x_{\mathbf{m}}[n]$ is defined as

$$x_{\mathbf{m}}[n] = i[n]^{|S_{\mathbf{m}}^1|} \cdot i[n-1]^{|S_{\mathbf{m}}^2|} \cdot q[n]^{|S_{\mathbf{m}}^3|} \cdot q[n-1]^{|S_{\mathbf{m}}^4|}.$$

From (13)-(16), it follows that $f_{\mathbf{m}}(t)$ can be written as

$$f_{\mathbf{m}}(t) = f_{m_1}^1(t) \cdot \ldots \cdot f_{m_d}^d(t) = \left(\sum_{r_c \in R_{\mathbf{m}}^c} \sum_{r_s \in R_{\mathbf{m}}^s} C_{r_c, r_s} \cdot e^{j\sigma(r_c, r_s)\omega_c t} \right) \sum_{n=-\infty}^{\infty} x_{\mathbf{m}}[n] p_{\mathbf{m},\tau}(t - nT), \tag{17}$$

where $\sigma([r_c^T, r_s^T]^T) = \sigma(r) = \sum_k r_c(k) + \sum_l r_s(l)$, and

$$C_{r_c, r_s} = \frac{(j)^{N_{\mathbf{m}}^2}}{2^d} \cdot e^{-j\omega_c[(r_c, \mathcal{P}_{\mathbf{m}}^1 \tau) + (r_s, \mathcal{P}_{\mathbf{m}}^2 \tau)]} \cdot \prod_{l=1}^{N_{\mathbf{m}}^2} r_s(l), \tag{18}$$
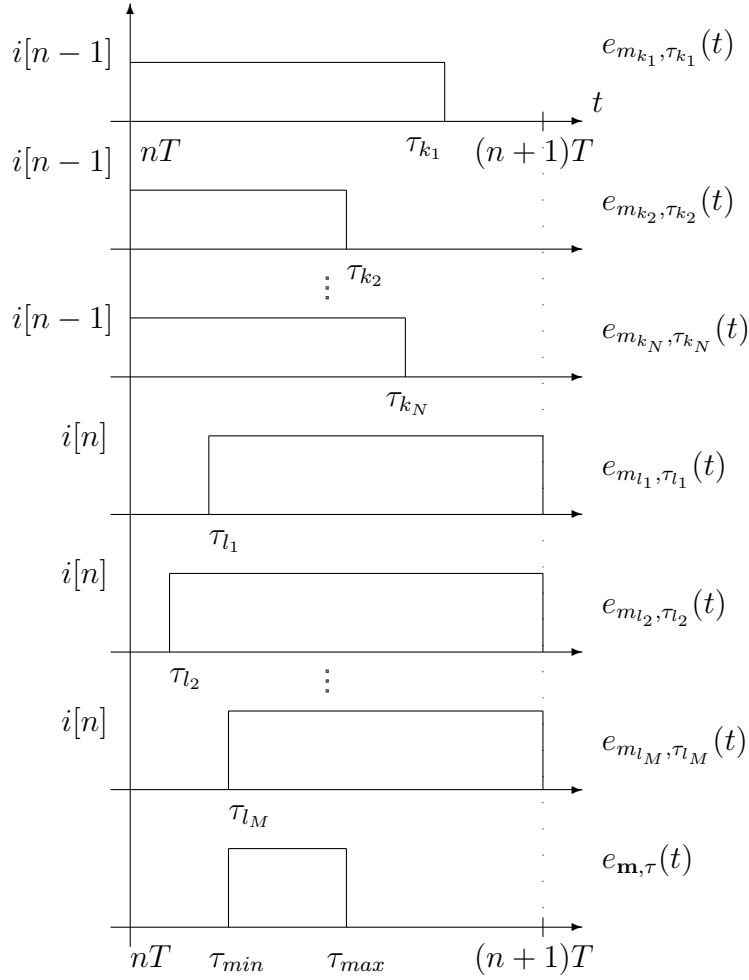
Figure 7: Signal $e_{\mathbf{m},\tau}$ for $S_{\mathbf{m}}^1 \cup S_{\mathbf{m}}^3 = \{k_1, k_2, \ldots, k_N\}$ and $S_{\mathbf{m}}^2 \cup S_{\mathbf{m}}^4 = \{l_1, l_2, \ldots, l_M\}$, where $N + M = d$

depends only on $\mathbf{m}$. Therefore, the output signal y of system $\mathbf{F}_\tau \mathbf{M}$, can be expressed in terms of w (more precisely in terms of i and q) by plugging the expression (17) for $f_{\mathbf{m}}(t)$ into (12). Thus we have found an explicit input-output relationship of system $\mathbf{F}_\tau \mathbf{M}$, which concludes the first part of the proof.

In order to find the relationship between input and output signals of the subsystem $\mathbf{DH}$, i.e. y and v, respectively, we first express signal u as a function of y (see Fig. 4). Recall that $u = \tilde{\mathbf{D}} y = \mathbf{EH_0 X_c H} y$. Let $U(\Omega)$ and $Y(\omega)$ denote the Fourier transforms of signals $u[n]$ and $y(t)$ respectively. Also let $H(\omega)$ and $H_0(\omega)$ be the frequency responses of ideal band-pass and

low-pass filters $\mathbf{H}$ and $\mathbf{H_0}$, given by

$$
\begin{aligned}
H(\omega) &= \begin{cases} 1, & \omega_c - \pi/T \leq |\omega| \leq \omega_c + \pi/T \\ 0, & \text{o/w} \end{cases}, \\
H_0(\omega) &= \begin{cases} 1, & |\omega| \leq \pi/T \\ 0, & \text{o/w} \end{cases}.
\end{aligned}
\tag{19}
$$

The following sequence of equalities holds

$$
\begin{aligned}
\mathcal{F}\{\mathbf{H}y\} &= Y(\omega)H(\omega), \\
\mathcal{F}\{\mathbf{X_c}\mathbf{H}y\} &= Y(\omega + \omega_c)H(\omega + \omega_c), \\
\mathcal{F}\{\mathbf{H_0}\mathbf{X_c}\mathbf{H}y\} &= Y(\omega + \omega_c)H(\omega + \omega_c)H_o(\omega), \\
U(\Omega) &= Y\left(\frac{\Omega}{T} + \omega_c\right) H\left(\frac{\Omega}{T} + \omega_c\right) H_0\left(\frac{\Omega}{T}\right).
\end{aligned}
$$

From the definition of $H(\omega)$ and $H_0(\omega)$, $U(\Omega)$ simplifies to

$$
U(\Omega) = Y\left(\frac{\Omega}{T} + \omega_c\right).
\tag{20}
$$

Equation (20) gives frequency domain relationship between y and u.

Next we express $Y(\omega)$ in terms of $X_{\mathbf{m}}(\Omega) = \mathcal{F}\{x_{\mathbf{m}}[n]\}$. For the sake of simplicity, we assume that $y(t)$ is equal to just one signal $f_{\mathbf{m}}(t)$ for some fixed $\mathbf{m}$, i.e. we omit the sum in (12). It follows from (17) that

$$
\mathcal{F}\{f_{\mathbf{m}}(t)\} = Y(\omega) = \sum_{r_c \in R_{\mathbf{m}}^c} \sum_{r_s \in R_{\mathbf{m}}^s} C_{r_c, r_s} X_{\mathbf{m}}\left(\omega T - \sigma(r) \cdot \omega_c T\right) P_{\mathbf{m}, \tau}\left(\omega - \sigma(r) \cdot \omega_c\right).
$$

Since $\sigma(r) \in \mathbb{Z}$ and $\omega_c T = 2\pi n$, where $n \in \mathbb{Z}$, we get

$$
Y(\omega) = X_{\mathbf{m}}(\omega T) \cdot \sum_{r_c \in R_{\mathbf{m}}^c} \sum_{r_s \in R_{\mathbf{m}}^s} C_{r_c, r_s} P_{\mathbf{m}, \tau}\left(\omega - \sigma(r) \cdot \omega_c\right).
\tag{21}
$$

It follows from (20) and (21) that

$$
U(\Omega) = X_{\mathbf{m}}(\Omega) \cdot \sum_{r_c \in R_{\mathbf{m}}^c} \sum_{r_s \in R_{\mathbf{m}}^s} C_{r_c, r_s} P_{\mathbf{m}, \tau}\left(\frac{\Omega}{T} - \omega_c \cdot \sigma(r) + \omega_c\right),
$$

with C_{r_c, r_s} as given in (18).

Therefore, the frequency response $G_{\mathbf{m}}(\Omega)$ of a LTI system mapping $x_{\mathbf{m}}$ to u is given by

$$
G_{\mathbf{m}}(\Omega) = \sum_{r_c \in R_{\mathbf{m}}^c} \sum_{r_s \in R_{\mathbf{m}}^s} C_{r_c, r_s} P_{\mathbf{m}, \tau}\left(\frac{\Omega}{T} - \omega_c \cdot \sigma(r) + \omega_c\right).
$$

This concludes the proof of Lemma 4.2. □

In Lemma 4.2, it was assumed that $\tau_i \in [0, T)$, $\forall i \in [d]$, but in general τ_i can take any positive real value depending on the depth of (2), i.e. vector $\mathbf{k}$ associated with τ is not necessarily zero vector. Suppose now that $\tau = \mathbf{k}T + \bar{\tau}$, where $\bar{\tau} \in [0, T)^d$, and $\mathbf{k} \neq \mathbf{0}$. In the rest of this proof we adopt the same notation for corresponding signals and systems as in the proof of Lemma 4.2.

Clearly, mapping from y to u is identical to the one derived for $\tau \in [0, T)$. Thus, in order to prove the statement of Theorem 4.1 we only have to find relationship between w and y. Let $d = 1$, i.e. $\tau = kT + \bar{\tau}$, with $k \in \mathbb{N}$ and $\bar{\tau} \in [0, T)$. Analogously to the case in the proof of Lemma 4.2, it follows that signal y can be expressed as

$$y(t) = [e_{1,\tau}(t) + e_{2,\tau}(t)] \cos(\omega_c t - \omega_c \tau) + [e_{3,\tau}(t) + e_{4,\tau}(t)] \sin(\omega_c t - \omega_c \tau),$$

where

$$e_{1,\tau} = \mathbf{Z_1}\mathbf{B}^{k+1}i, \quad \text{i.e.,} \quad e_{1,\tau}(t) = \frac{1}{T} \sum_{n=-\infty}^{\infty} i[n - k - 1]p_{1,\bar{\tau}}(t - nT),$$

$$e_{2,\tau} = \mathbf{Z_2}\mathbf{B}^{k}i, \quad \text{i.e.,} \quad e_{2,\tau}(t) = \frac{1}{T} \sum_{n=-\infty}^{\infty} i[n - k]p_{2,\bar{\tau}}(t - nT),$$

$$e_{3,\tau} = \mathbf{Z_1}\mathbf{B}^{k+1}q, \quad \text{i.e.,} \quad e_{3,\tau}(t) = -\frac{1}{T} \sum_{n=-\infty}^{\infty} q[n - k - 1]p_{1,\bar{\tau}}(t - nT),$$

$$e_{4,\tau} = \mathbf{Z_2}\mathbf{B}^{k}q, \quad \text{i.e.,} \quad e_{4,\tau}(t) = -\frac{1}{T} \sum_{n=-\infty}^{\infty} q[n - k]p_{2,\bar{\tau}}(t - nT).$$

(22)

Here $\mathbf{B}^k$ denotes the composition of $\mathbf{B}$ with itself k times, i.e. $\mathbf{B}^k : x[n] \mapsto y[n] = x[n - k]$.

For $d > 1$, reasoning similar to that in the proof of Lemma 4.2, leads to the following expression for $e_{\mathbf{m},\tau}$:

$$e_{\mathbf{m},\tau}(t) = \sum_{n=-\infty}^{\infty} x_{\mathbf{m},\mathbf{k}}[n]p_{\mathbf{m},\bar{\tau}}(t - nT),$$

(23)

where

$$x_{\mathbf{m},\mathbf{k}}[n] = \prod_{i \in S_{\mathbf{m}}^1} i[n - k_i - 1] \cdot \prod_{i \in S_{\mathbf{m}}^2} i[n - k_i] \cdot \prod_{i \in S_{\mathbf{m}}^3} q[n - k_i - 1] \cdot \prod_{i \in S_{\mathbf{m}}^4} q[n - k_i],$$

and $p_{\mathbf{m},\bar{\tau}}(t)$ is defined in (4). Let $X_{\mathbf{m},\mathbf{k}} = X_{\mathbf{m},\mathbf{k}}(\Omega)$ be the Fourier transform of $x_{\mathbf{m},\mathbf{k}}$. With (23) at hand, it is straightforward to find the analytic expression for $U = \mathcal{F}u$, in terms of $X_{\mathbf{m},\mathbf{k}}$. Similarly to (17)-(21), the Fourier transform $Y = \mathcal{F}y$, can be written as

$$Y(\omega) = X_{\mathbf{m},\mathbf{k}}(\omega T) \cdot \sum_{r_c \in R_{\mathbf{m}}^c} \sum_{r_s \in R_{\mathbf{m}}^s} C_{r_c,r_s} P_{\mathbf{m},\bar{\tau}} (\omega - \sigma(r) \cdot \omega_c),$$

(24)

where

$$C_{r_c,r_s} = \frac{(j)^{N_{\mathbf{m}}^2}}{2^d} \cdot e^{-j\omega_c [(r_c, \mathcal{P}_{\mathbf{m}}^1 \bar{\tau}) + (r_s, \mathcal{P}_{\mathbf{m}}^2 \bar{\tau})]} \cdot \prod_{l=1}^{N_{\mathbf{m}}^2} r_s(l),$$

(25)

It follows from (20) and (24) that

$$U(\Omega) = X_{\mathbf{m,k}}(\Omega) \cdot \sum_{r_c \in R^c_{\mathbf{m}}} \sum_{r_s \in R^s_{\mathbf{m}}} C_{r_c, r_s} P_{\mathbf{m}, \bar{\tau}} \left(\frac{\Omega}{T} - \omega_c \cdot \sigma(r) + \omega_c \right).$$

Statement of the Theorem now imediatelly proceeds from the above equality. This concludes the proof.

□

Block diagram of system $\mathbf{S}_\tau = \mathbf{DHF}_\tau \mathbf{M}$, as suggested in the statement of Theorem 4.1, is shown in Fig. **??**. System $\mathbf{S}_\tau$ can be represented as a parallel interconnection of DT nonlinear Volterra subsystems $\mathbf{V_{m,k}}$ mapping input signal w into output signal $x_{\mathbf{m,k}}$, and DT LTI systems $\mathbf{G_{m,k}}$ mapping input signal $x_{\mathbf{m,k}}$ into output signal $u_{\mathbf{m}}$.

5 Discussion

5.1 Effects of oversampling

The analytical result of this paper suggests a special structure of a digital pre-distortion compensator which appears to be, in first approximation, both necessary and sufficient to match the discrete time dynamics resulting from combining modulation and demodulation with a dynamic non-linearity in continuous time. The "necessity" somewhat relies on the input signal u having "full" spectrum. In digital communications it is very common practice to oversample baseband signal (symbols), and shape its spectrum (samples), before it is modulated onto a carrier [21]. In the case of large oversampling ratios, from symbol to sample space, the effective band of the signal containing symbol information is small compared to the band assigned by the regulatory agency. So in order to transmit symbol information without distortion, the reconstruction filter has to match the frequency response of the ideal baseband model LTI filter only on this effective band (and the rest can be zeroed-out by applying a smoothing filter after demodulation). This now allows for reconstruction filters in baseband equivalent model to be not just smooth, but also continuous, and thus well approximable by short memory FIR filters. This in turn implies that the plain Volterra structure with relatively short memory can capture dynamics of such system well enough, possibly diminishing the need for any special models. While, theoretically, the baseband signal u is supposed to be shaped so that only a lower DT frequency spectrum of it remains significant (i.e. oversampling is employed), a practical implementation of amplitude-phase modulation will frequently employ a signal component separation approach, such as LINC [22], where the low-pass signal u is decomposed into two components of constant amplitude, $u = u_1 + u_2$, $|u_1[n]| \equiv |u_2[n]| = \text{const}$, after which the components u_i are fed into two separate modulators, to produce continuous time outputs y_1, y_2, to be combined into a single output $y = y_1 + y_2$. Even when u is band-limited, the resulting components u_1, u_2 are not, and the full range of modulator's nonlinearity is likely to be engaged when producing y_1 and y_2. Also in high-speed wideband communication systems, the oversampling ratio is usually limited by the speed that the digital baseband and DAC are able to sustain, therefore the latter

scenario described is usually encountered and the compensator model should be able to take care of this factor.

5.2   Extension to OFDM

Orthogonal frequency-division multiplexing (OFDM) is a multicarrier digital modulation scheme that has been the dominant technology for broadband multicarrier communications in the last decade. Compared with single-carrier digital modulation, by increasing the effective symbol length and employing many carriers for transmission, OFDM theoretically eliminates the problem of multi-path channel fading, which is the main type of disturbance on a terrestrial transmission path. It also mitigates low spectrum efficiency, impulse noise, and frequency selective fading [21, 23]. One of the major drawbacks of OFDM is the relatively large Peak-to-Average Power Ratio (PAPR) [24]. This makes OFDM very sensitive to the nonlinear distortion introduced by high PA, which causes in-band as well as out-of-band (i.e. adjacent channel) radiation, decreasing spectral efficiency [25]. For that reason linearization techniques play very important role in OFDM, and have been studied extensively [26]-[28].

Fig. 8 shows a block diagram of the typical implementation of an N-carrier OFDM system. Input stream of symbols $u[n]$, with bandwidth B, is first converted into blocks of lenght N by serial-to-parallel conversion, which are then fed to an N-point inverse FFT block. Output of this block is then transformed with a parallel-to-serial converter into a stream of N samples $v[k]$, with bandwidth B (usually this bandwidth is larger than the input symbols' bandwidth, but in our discussion we ignore introduction of the guard interval (i.e. addition of cyclic redundancy), which is usually used to mitigate the impairments of the multipath radio channel, as it does not affect aplicability of the baseband model and the DPD proposed in this paper). Digital-to-analog convertion is then applied to $w[k]$, and its output is used to modulate a single carrier. As can be seen from Figure 8, sequence $w[k]$ can be seen as an input to a system which can be modeled as the **DHFM** system investigated in the previous chapter. In our derivation of the baseband model, choice of the input symbols' values (e.g. QPSK, QAM, etc.), was not relevant to the actual derivation. In other words, input symbols can take any value from $\mathbb{C}$, hence sequence $w[k]$ can be considered as a legitimate input sequence to a system modeled as **DHFM**. This suggests that our baseband model, and its corresponding DPD structure, can be possibly used for distortion reduction in OFDM modulation applications.

6   Simulation Results

In this section, aided by MATLAB simulations, we illustrate performance of the proposed compensator structure. We compare this structure with some standard compensator structures, together with the ideal compensator, and show that it closely resembles dynamics of ideal compensator, thus achieving near optimal compensation performance.

The underlying system $\mathbf{S}$ is shown in Figure 1, with the analog channel subsystem $\mathbf{F}$ given by

$$(Fx)(t) = x(t) - \delta \cdot x(t - \tau_1)x(t - \tau_2)x(t - \tau_3), \tag{26}$$
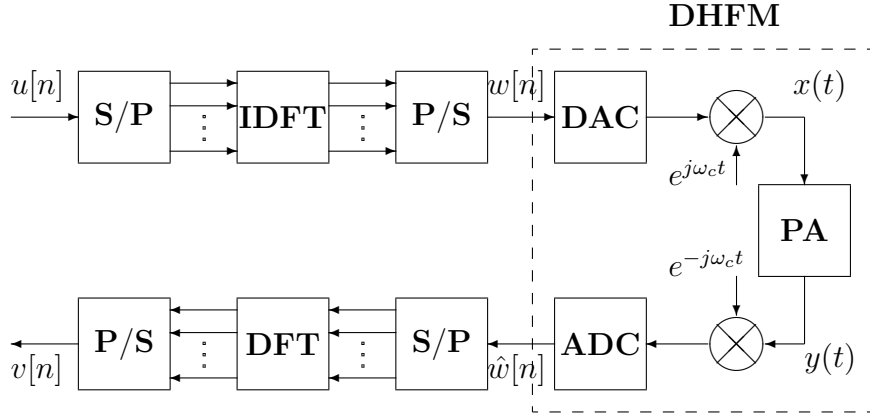
Figure 8: Block diagram of a typical implementation of OFDM

where $0 \leq \tau_1 \leq \tau_2 \leq \tau_3 \leq T$, with T sampling time, and $\delta > 0$ parameter specifying magnitude of distortion $\boldsymbol{\Delta}$ in $\mathbf{S} = \mathbf{I} + \boldsymbol{\Delta}$. We assume that parameter δ is relatively small, in particular $\delta \in (0, 0.2)$, so that the inverse $\mathbf{S}^{-1}$ of $\mathbf{S}$ can be well approximated by $2\mathbf{I} - \mathbf{S}$. Then our goal is to build compensator $\mathbf{C} = \mathbf{S}^{-1}$ with different structures, and compare their performance, which is measured as output Error Vector Magnitude (EVM) [3] defined, for a given input-output pair $(u, \hat{u})$, as

$$\text{EVM(dB)} = 20 \log_{10} \left(\frac{||u - \hat{u}||_2}{||u||_2} \right).$$

Analytical results from the previous section suggest that the compensator structure should be of the form depicted in Figure 2. It is easy to see from the proof of Theorem 4.1, that transfer functions in $\mathbf{L}$, from each nonlinear component $g_k[n]$ of $g[n]$, to the output $v[n]$, are smooth functions, hence can be well approximated by low order polynomials in Ω. In this example we choose second order polynomial approximation of components of $\mathbf{L}$. This observation, together with the true structure of $\mathbf{S}$, suggests that compensator $\mathbf{C}$ should be fit within a family of models with structure shown on the block diagram in Fig 9, where

(a) Subsystems $\mathbf{H}_i, i = 1, 2, 3$, are LTI systems, with transfer functions H_i given by

$$H_0(e^{j\Omega}) = 1, H_1(e^{j\Omega}) = j\Omega, H_2(e^{j\Omega}) = \Omega^2, \forall \Omega \in [-\pi, \pi].$$

(b) The nonlinear subsystems $\mathbf{V}_i$ are modeled as third order Volterra series, with memory $m = 1$, i.e.

$$(\mathbf{V}_j w)[n] = \sum_{(\alpha(k), \beta(k))} c_k^j \prod_{l=0}^{1} i[n-l]^{\alpha_l(k)} \prod_{l=0}^{1} q[n-l]^{\beta_l(k)},$$

$$\alpha_l(k), \beta_l(k) \in \mathbb{Z}_+, \qquad \sum_{l=0}^{1} \alpha_l(k) + \sum_{l=0}^{1} \beta_l(k) \leq 3,$$
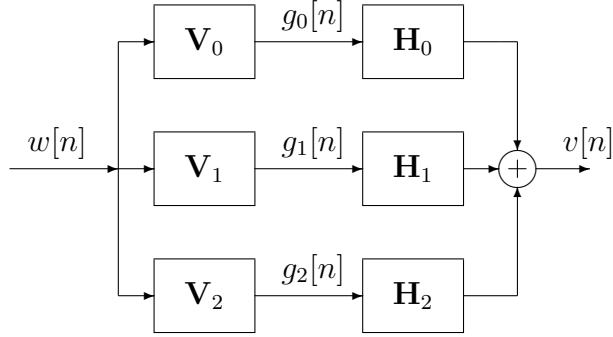
Figure 9: Proposed compensator structure

where $i[n] = \mathrm{R}e\, w[n]$ and $q[n] = \mathrm{I}m\, w[n]$, and $(\alpha(k), \beta(k)) = (\alpha_0(k), \alpha_1(k), \beta_0(k), \beta_1(k))$.

We compare performance of this compensator with the widely used one obtained by utilizing simple Volterra series structure [3]:

$$(\mathbf{K}w)[n] = \sum_{(\alpha(k), \beta(k))} c_k \prod_{l=-m_1}^{m_2} i[n-l]^{\alpha_l(k)} \prod_{l=-m_1}^{m_2} q[n-l]^{\beta_l(k)},$$

$$\alpha_l(k), \beta_l(k) \in \mathbb{Z}_+, \qquad \sum_{l=-m_1}^{m_2} \alpha_l(k) + \sum_{l=-m_1}^{m_2} \beta_l(k) \leq d.$$

Parameters of $\mathbf{K}$ which could be varied are forward and backward memory depth m_1 and m_2, respectively, and degree d of this model. We consider three cases for different sets of parameter values:

- Case 1: $m_1 = 0$, $m_2 = 2$, $d = 5$

- Case 2: $m_1 = 0$, $m_2 = 4$, $d = 5$

- Case 3: $m_1 = 2$, $m_2 = 2$, $d = 5$

Table 1: Number of coefficients c_k being optimized for different compensator models

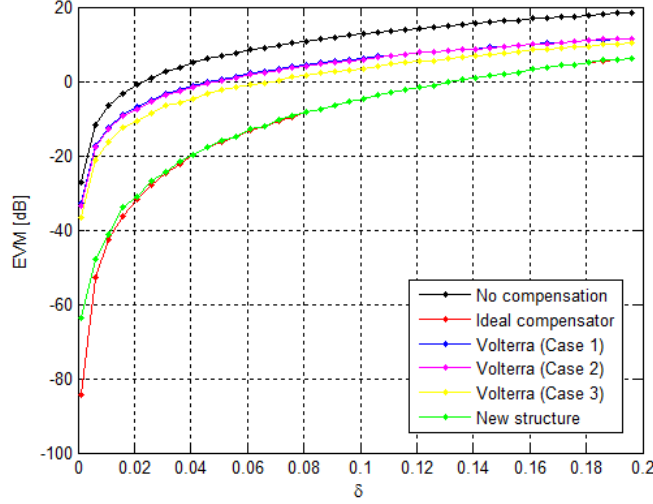| Model	# of c_k	# of significant c_k
New structure	210	141
Volterra 1	924	177
Volterra 2	6006	2058
Volterra 3	6006	1935

Figure 10: Output EVM for different compensator structures

After fixing the compensator structure, coefficients c_k are obtained by applying straightforward least squares optimization.
We should emphasize here that fitting has to be done for both real and imaginary part of $v[n]$, thus the actual compensator structure is twice that depicted in Figure 9.

Simulation parameters for system $\mathbf{S}$ are as follows: symbol rate $f_{symb} = 2\text{MHz}$, carrier frequency $f_c = 20\text{MHz}$, with 64QAM input symbol sequence. Nonlinear distortion subsystem $\mathbf{F}$ of $\mathbf{S}$, used in simulation, is defined in (26), where the delays τ_1, τ_2, τ_3 are given by the vector $\tau = [0.2T \quad 0.3T \quad 0.4T]$, with $T = 1/f_{symb}$. Digital simulation of the continuous part of $\mathbf{S}$ was done by representing continuous signals by their discrete counterparts, obtained by sampling with high sampling rate $f_s = 1000 \cdot f_{symb}$. We use a 64QAM symbol sequence, with period $N_{symb} = 4096$, as an input to $\mathbf{S}$. This period length is used for generating input/output data for fitting coefficients c_k, as well as generating input/output data for performance validation.
In Figure 10 we present EVM obtained for different compensator structures, as well as output EVM with no compensation, and case with ideal compensator $\mathbf{C} = \mathbf{S}^{-1} \approx 2\mathbf{I} - \mathbf{S}$. As can be seen from Figure 10, compensator fitted using the proposed structure in Figure 9 outperforms other compensators, and gives output EVM almost identical to the ideal compensator. This result was to be expected, since model in Figure 9 approximates the original system $\mathbf{S}$ very closely, and thus is capable of approximating system $2\mathbf{I} - \mathbf{S}$ closely as well. This is not the case for compensators modeled with simple Volterra series, due to inherently long (or more precisely infinite) memory introduced by the LTI part of $\mathbf{S}$. Even if we use noncausal Volterra series model (i.e. $m_1 \neq 0$), which is expected to capture true dynamics better, we are still unable to get good fitting of the system $\mathbf{S}$, and consequently of the compensator $\mathbf{C} \approx 2\mathbf{I} - \mathbf{S}$.
Advantage of the proposed compensator structure is not only in better compensation performance, but also in that it achieves better performance with much more efficient strucure. That

is, we need far less coefficients in order to represent nonlinear part of the compensator, in both least squares optimization and actual implementation (Table 1). In Table 1 we can see a comparison in the number of coefficients between different compensator structures, for nonlinear subsystem parameter value $\delta = 0.02$. Data in the first column is number of coefficients (i.e. basis elements) needed for general Volterra model, i.e. coefficients which are optimized by least squares. The second column shows actual number of coefficients used to build compensator. Least squares optimization yields many nonzero coefficients, but only subset of those are considered significant and thus used in actual compensator implementation. Coefficient is considered significant if its value falls above a certain treshold t, where t is chosen such that increase in EVM after zeroing nonsignificant coefficients is not larger than 1% of the best achievable EVM (i.e. when all basis elements are used for building compensator). From Table 1 we can see that for case 3 Volterra structure, 10 times more coefficients are needed in order to implement compensator, than in the case of our proposed structure. And even when such a large number of coefficients is used, its performance is still below the one achieved by this new compensator model.

7 Conclusion

In this paper, we propose a novel explicit expression of the equivalent baseband model, under assumption that the passband nonlinearity can be described by a Volterra series model with the fixed degree and memory depth. This result suggests a new, non-obvious, analytically motivated structure of digital precompensation of passband nonlinear distortions caused by power amplifiers, in digital communication systems. It has been shown that the baseband equivalent model is a series connection of a fixed degree and short memory Volterra model, and a long memory discrete-time LTI system, called reconstruction filter. Frequency response of the reconstruction filter is shown to be smooth, hence well aproximable by low order polynomials. Parameters of such a model (and accordingly of the predistorter) can be obtained by applying simple least squares optimization to the input/output data measured from the system, thus implying low implementation complexity. State of the art implementations of DPD, have long memory requirements in the nonlinear subsystem, but structure of our baseband equivalent model suggests that the long memory requirements can be shifted from the nonlinear part to the LTI part, which consists of FIR filters and is easy to implement in digital circuits, giving it advantage of much lower complexity. We also argued that this baseband model, and its corresponding DPD structure, can be readily extended to OFDM modulation. Simulation results have shown that by using this new DPD structure, significant reduction in nonlinear distortion caused by the RF PA can be achieved, while utilizing full frequency band, and thus effectively using maximal input symbol rate.

References

[1] P. B. Kennington, *High linearity RF amplifier design*. Norwood, MA: Artech House, 2000.

[2] S. C. Cripps, *Advanced techniques in RF power amplifier design*. Norwood, MA: Artech House, 2002.

[3] J. Vuolevi, and T. Rahkonen, *Distortion in RF Power Amplifiers*. Norwood, MA: Artech House, 2003.

[4] A. A. M. Saleh, and J. Salz, "Adaptive linearization of power amplifiers in digital radio systems," *Bell Syst. Tech. J.*, vol. 62, no. 4, pp. 1019-1033, April 1983.

[5] W. Bösch, and G. Gatti, "Measurement and simulation of memory effects in predistortion linearizers," *IEEE Trans. Microw. Theory Techn.*, vol. 37, pp. 1885-1890, December 1989.

[6] J. Kim, and K. Konstantinou, "Digital predistortion of wideband signals based on power amplifier model with memory," *Electron. Lett.*, vol 37, no. 23, pp. 1417-1418, November 2001.

[7] L. Ding, G. T. Zhou, D. R. Morgan, Z. Ma, J. S. Kenney, J. Kim, and C. R. Giardina, "A robust digital baseband predistorter constructed using memory polynomials," *IEEE Trans. Commun.*, vol. 52, no. 1, pp.159-165, January 2004.

[8] V. J. Mathews and G. L. Sicuranza, *Polynomial Signal Processing*. New York: Wiley, 2000.

[9] A. Zhu, and T. Brazil, "Behavioral modeling of RF power amplifiers based on pruned Volterra series," *IEEE Microw. Wireless Compon. Lett.*, vol. 14, no. 12, pp. 563-565, December 2004

[10] D. R. Morgan, Z. Ma, J. Kim, M. Zierdt, and J. Pastalan, "A generalized memory polynomial model for digital predistortion of RF power amplifiers," *IEEE Trans. Signal Process.*, vol. 54, no. 10, pp. 3852-3860, October 2006.

[11] A. Zhu, J. C. Pedro, and T. J. Brazil, "Dynamic deviation reduction-based Volterra behavioral modeling of RF power amplifiers," *IEEE Trans. Microw. Theory Techn.*, vol. 54, No. 12, pp. 4323-4332., December 2006.

[12] A. Zhu, P. J. Draxler, J. J. Yan, T. J. Brazil, D. F. Kimball, and P. M. Asbeck, "Open-loop digital predistorter for RF power amplifiers using dynamic deviation reduction-based Volterra series," *IEEE Trans. Microw. Theory Techn.*, vol. 56, No. 7, pp. 1524-1534., July 2008.

[13] M. Rawat, K. Rawat, and F. M. Ghannouchi, "Adaptive digital predistortion of wireless power amplifiers/transmitters using dynamic real-valued focused time-delay line neural networks," *IEEE Trans. Microw. Theory Techn.*, vol. 58, No. 1, pp. 95-104, January 2010.

[14] M. Rawat, K. Rawat, F. M. Ghannouchi, S. Bhattacharjee, and H. Leung, "Generalized rational functions for reduced-complexity behavioral modeling and digital predistortion of broadband wireless transmitters," *IEEE Trans. Instrum. Meas.*, vol. 63, No. 2, pp. 485-498, February 2014.

[15] C. Yu, L. Guan, and A. Zhu, "Band-Limited Volterra Series-Based Digital Predistortion for Wideband RF Power Amplifiers," *IEEE Trans. Microw. Theory Techn.*, vol. 60, No. 12, pp. 4198-4208, December 2012.

[16] O. Tanovic, R. Ma, and K. H. Teo, "Novel Baseband Equivalent Models of Quadrature Modulated All-Digital Transmitters," *Radio Wireless Symposium (RWS) 2017*, Phoenix, AZ, 15-17 Jan. 2017

[17] G. M. Raz, and B. D. Van Veen, "Baseband Volterra filters for implementing carrier based nonlinearities," *IEEE Trans. Signal Process.*, vol. 46, no. 1, pp. 103-114, January 1998.

[18] M. Schetzen, *The Volterra and Wiener theories of nonlinear systems*. reprint ed. Malabar, FL: Krieger, 2006.

[19] W. Frank, "Sampling requirements for Volterra system identification," *IEEE Signal Process. Lett.*, vol. 3, no. 9, pp. 266-268, September 1996

[20] J.Tsimbinos, and K.V.Lever, "Input Nyquist sampling suffices to identify and compensate nonlinear systems," *IEEE Trans. Signal Process.*, vol. 46, no. 10, pp. 2833-2837, Oct. 1998.

[21] J. G. Proakis and M. Salehi, *Digital Communications*. McGraw-Hill, 2007

[22] D. C. Cox, "Linear amplification with nonlinear components," *IEEE Trans. Commun.*, vol. 22, no. 12, pp. 1942-1945, Dec. 1974.

[23] A. Goldsmith, *Wireless Communications*. Cambridge University Press, 2005.

[24] S. H. Han and J. H. Lee, "An overview of peak-to-average power ratio reduction techniques for multicarrier transmission," *IEEE Wireless Commun.*, vol. 52, pp. 5-65, March 2005

[25] Q. Shi, "OFDM in bandpass nonlinearity," *IEEE Trans. Consumer Electron.*, vol. 42, pp. 253-258, August 1996.

[26] A. N. D'Andrea, V. Lottici, and R. Reggiannini, "Nonlinear predistortion of OFDM signals over frequency-selective fading channels," *IEEE Trans. Commun.*, vol. 49, no. 5, pp. 837-843, May 2001.

[27] F. Wang; D.F. Kimball, D.Y. Lie, P.M. Asbeck, and L. E. Larson, "A Monolithic High-Efficiency 2.4-GHz 20-dBm SiGe BiCMOS Envelope-Tracking OFDM Power Amplifier," *IEEE J. Solid-State Circuits*, vol.42, no.6, pp.1271,1281, June 2007.

[28] J. Reina-Tosina, M. Allegue-Martinez, C. Crespo-Cadenas, C. Yu, and S. Cruces, "Behavioral Modeling and Predistortion of Power Amplifiers Under Sparsity Hypothesis," *IEEE Trans. Microw. Theory Techn.*, vol. 63, no. 2, pp. 745-753, February 2015.

[29] O. Tanovic, A. Megretski, Y. Li ,V. M. Stojanovic and M. Osqui, "Discrete-time models resulting from dynamic continuous-time perturbations in phase-amplitude modulation-demodulation schemes," *2016 IEEE 55th Conference on Decision and Control (CDC)*, Las Vegas, NV, 2016, pp. 6619-6624.